Forest Ecology and Management 580 (2025) 122546

Contents lists available at ScienceDirect

Forest Ecology and Management

journal homepage: www.elsevier.com/locate/foreco

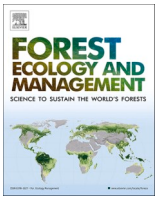

Ongoing regeneration of ash and co-occurring species 20 years following invasion by emerald ash borer

Caleb J. Wilson [a,*,1], Louise Labbate [b], Toby R. Petrice [b], Therese M. Poland [b], Deborah G. McCullough [a,c]

[a] Department of Entomology, Michigan State University, East Lansing, MI, USA
[b] US. Department of Agriculture, Forest Service, Northern Research Station. East Lansing, MI, USA
[c] Department of Forestry, Michigan State University, East Lansing, MI, USA

ARTICLE INFO

Keywords:
Ash regeneration
Emerald ash borer
Forest community composition
Fraxinus
Invasive forest pest

ABSTRACT

Emerald ash borer (*Agrilus planipennis* Fairmare) is a destructive invasive insect pest of ash trees (*Fraxinus* spp.) in North America. Monitoring ash regeneration within post-invasion forests is essential to assess ash persistence in North America. We recorded density of overstory ash [> 10 cm diameter at breast height (DBH)], ash recruits (2–10 cm DBH), ash saplings (≥ 45 cm in height; < 2 cm DBH), and ash seedlings (< 45 cm in height), along with canopy dieback of overstory ash and recruits in four post-invasion areas in south-central Michigan, USA. We also recorded density of all other overstory trees, recruits, saplings, and seedlings by species. Ash regeneration was abundant in recruit (470 ± 68.9 stems per ha), sapling (2599 ± 336.1 stems per ha), and seedling strata (4557 ± 557.9 stems per ha). Overall, 47 % of overstory ash, 17 % of ash recruits, and 7 % of ash saplings were dead. More than half of the live overstory ash (54 %), and 43 % of ash recruits had < 30 % dieback, although 33 ± 3.0 % of ash recruits had external signs of EAB infestation. Living ash basal area was inversely associated with *Quercus rubra* and *Tilia americana* density. Dead ash basal area was not related to tree species composition, indicating that stands with low ash density, and subsequent effects on community structure, were not due to canopy gaps resulting from EAB mortality. Overall, we documented substantial ash regeneration in post-invasion forests despite high mortality of trees > 10 cm DBH.

1. Introduction

Emerald ash borer (EAB), (*Agrilus planipennis* Fairmare), is the most destructive insect forest pest to invade North America (Aukema et al., 2011, Herms and McCullough, 2014, McCullough, 2020). Widespread mortality of ash in North America has resulted in numerous effects on ecosystems where ash was a dominant species. Loss of overstory ash has altered local hydrology, nutrient cycles, as well as plant, insect, and wildlife communities (Flower et al., 2013; Nisbet et al., 2015; Engelken and McCullough, 2020a,b; Grinde et al., 2022; Herms and McCullough, 2014; Klooster et al., 2018; Kolka et al., 2018; Krzemien et al., 2024, Larson et al., 2022; McCullough, 2020). In studies conducted in southeast Michigan and northeast Ohio during the decade following the initial EAB invasion in the early 2000s, ash seedlings and saplings were less abundant in forest stands where EAB had caused overstory ash decline (Kashian and Witter, 2011; Klooster et al., 2014). Rates of overstory ash mortality during this period were typically above 80 % and could be as high as 99 % (Burr and McCullough, 2014; Engelken et al., 2020; Klooster et al., 2014; Knight et al., 2013; Siegert et al., 2021; Smith et al., 2015).

Since the initial invasion and spread of EAB, recent surveys of ash prevalence in forests in southern Michigan have documented higher survival of certain ash species than previously expected. For example, when Robinett and McCullough (2019) surveyed ash in 24 forests, primarily in southeast Michigan in 2015, 75 % of white ash (*Fraxinus americana* L.) trees between 10 and 44 cm DBH were alive, while 92 % of all green ash (*F. pennyslvanica* Marshall) overstory trees were dead. In contrast, Siegert et al. (2021) surveyed green ash and black ash (*F. nigra* Marshall) in forests of northern and central Michigan in 2007–2008 before forests were colonized by EAB, and then again a decade later. In post-invasion forests, virtually all green ash and black ash trees > 13 cm DBH were dead and the only live ash in these forests was represented by

* Corresponding author.
E-mail address: c.wilson@uky.edu (C.J. Wilson).
[1] Present address: Department of Entomology, University of Kentucky, Lexington, KY. USA.

https://doi.org/10.1016/j.foreco.2025.122546
Received 26 November 2024; Received in revised form 15 January 2025; Accepted 28 January 2025
Available online 2 February 2025

small saplings and seedlings (Siegert et al., 2021). Studies conducted in forests containing both blue ash (*F. quadrangulata* Michx.) and white ash in Michigan and Ohio found far higher mortality of white ash in comparison to blue ash, yet white ash continued to regenerate in these forests (Cipollini and Morton, 2023; Spei and Kashian, 2017; Tanis and McCullough, 2012). Variable effects of EAB invasion on ash mortality reflects differences in EAB host preference and vulnerability of native ash species. Tanis and McCullough (2015) compared adult EAB leaf feeding and larval densities among black, green, white, blue, and Manchurian ash (*F. mandshurica* Ruprecht) in a common garden experiment. Based on adult survival and larval densities, they found that Manchurian and blue ash were relatively resistant to EAB, black and green ash were highly vulnerable, and white ash was intermediate. These studies indicate that as EAB kills more of the preferred host species (e.g., black ash, green ash), less preferred species (white ash, blue ash) may become proportionally more abundant within the overstory. Despite high ash mortality since the arrival of EAB, ash persists in invaded forests and continues to regenerate, although small trees and saplings now represent most of the ash phloem area in many post-invasion forests (McCullough and Siegert, 2007, Siegert et al., 2021).

There have been several studies to understand and predict the degree to which ash decline may influence tree community composition in post-invasion forests. Burr and McCullough (2014) examined tree communities in 24 forests across an east to west gradient of EAB invasion: core (post-invasion), crest (recently invaded), and cusp (early-stage invasion) in southern Michigan. They found that canopy gaps caused by ash mortality in core sites were largely filled by lateral ingrowth of species such as American elm (*Ulmus americana* L.), black cherry (*Prunus serotina* Ehrh.), and northern red oak (*Quercus rubra* L.). However, regeneration strata were dominated by red maple (*Acer rubrum* L.), sugar maple (*A. saccharum* Marshall), and black cherry, suggesting that these species are poised to replace ash as dominant overstory species (Burr and McCullough, 2014). Similarly, Hoven et al. (2020) found complex responses of forests to EAB-induced ash mortality in 24 sites across three regions in Ohio. In general, they found mortality of overstory ash released non-ash trees, particularly maples, and increased abundance of maple and non-native tree and shrub seedlings. Marshall (2020) examined forest composition a decade after EAB invasion in 44 sites across Indiana, Michigan and Ohio. Green ash seedlings were abundant in the understory along with sugar maple, black, cherry and American elm, whereas overstory composition shifted to non-ash species, threatening the availability of ash seed sources. Red maple and sugar maple are shade tolerant and can establish in a wide range of soil conditions (Godman et al., 1990; Walters and Yawney, 1990), while black cherry is shade intolerant but, like ash, commonly colonizes canopy gaps (Marquis, 1990). Although Clark (1962) reported ash could persist in seed banks for more than three years, Klooster et al. (2014) determined viable ash seeds were low or scarce in seed banks sampled in southeast Michigan stands invaded by EAB. Nevertheless, live ash regeneration is commonly recorded in post-invasion forests despite high mortality of overstory ash (Aubin et al., 2015, Kashian, 2016; Abella et al., 2019; Marshall, 2020; Engelken and McCullough, 2020b; Engelken et al., 2020; Robinett and McCullough, 2019; Siegert et al., 2021). Given that trees as small as 2.5 cm in diameter can be colonized and killed by EAB (Cappaert et al., 2005), EAB-induced mortality of ash recruits may hinder the ability of ash to compete with other regenerating species and survive to reproductive ages.

Populations of EAB have declined in much of Michigan, reflecting the reduced carrying capacity in post-invasion stands (Siegert et al., 2021) and it is unclear how EAB population dynamics will influence ash persistence over time. Data collected by the USDA Forest Service Forest Inventory and Analysis program (FIA) in 2013–2018 indicated that forests invaded during assessments conducted from 2002 to 2006 had approximately 50 % higher ash mortality per ha than ash recruitment into the overstory, indicating ash recruits died at a faster rate than young trees recruited into the overstory (Ward et al., 2021).The young green and white ash present today in many post-invasion stands in Michigan were saplings when EAB first invaded and were likely too small to become infested at that time. Reduced EAB density in post-invasion forests may facilitate greater regeneration and recruitment of ash into the overstory canopy. However, EAB densities may build again in post-invasion forests as regenerating ash grow, which would limit recruitment of young trees to the overstory. It is therefore necessary to determine the extent to which ash are regenerating in post-invasion forests and which tree species fill canopy gaps created by ash decline.

We evaluated ash regeneration in four forests in south-central Michigan that were invaded by EAB approximately 15–20 years earlier. Our goal was to quantify ash survival, mortality, and regeneration of ash and other species in these post-invasion forests. We also evaluated how tree community composition at our sites was influenced by the prevalence of living and dead ash to identify tree species likely to replace ash in post-invasion forests.

2. Methods

2.1. Ash canopy condition

We quantified ash regeneration and tree species composition in south-central Michigan on four properties owned by the Michigan Department of Natural Resources including Muskrat Lake State Game Area (Clinton County), Rose Lake State Wildlife Area (Ingham County), Tamarack Lake State Game Area (Eaton County), and Sleepy Hollow State Park (Clinton County). We overlaid a 50 × 50 m grid across the entire extent of each property in ArcGIS Pro (ESRI 2023), then surveyed sites in May 2022 to identify grid cells where live ash trees were present. Results were mapped using Google Earth Pro 2022 (Google Inc. 2022) and grid cells lacking at least four live ash trees with DBH > 3 cm were excluded from further sampling.

Within each grid cell, we visually estimated canopy dieback and transparency of four randomly selected living ash trees. We recorded canopy dieback and transparency in 10 % increments, where a tree with 10 % dieback was healthy while a tree with 90 % dieback was nearly dead (Shoemaker et al., 2007, Smitley et al., 2008). Similarly, a tree with 10 % transparency has a nearly full crown while a tree with 90 % transparency has little live foliage. To select the first tree, we walked in a straight line from the center of each grid cell in a randomly selected direction, to a maximum distance of 18 m, until we encountered the first living ash tree (DBH > 3 cm). We then returned to the center of the cell and repeated this process in three additional directions in increments of 90 degrees. When no living ash trees were found along the transect within 18 m, we expanded our search to either side of the transect until a living ash could be located. If we could not locate four live ash trees with DBH > 3 cm, the cell was removed from the sampling protocol. Canopy condition of each tree was assessed once between early June and late August in both 2022 and 2023. In 2023, replacement trees were selected following the same protocol in cases where the monitoring trees in a cell had died, were felled by beavers, or could not be re-located. Between assessments conducted in 2022 and 2023, 38 trees were killed by EAB, and 26 trees died from other causes or could not be relocated.

2.2. Overstory and recruit surveys

In addition to evaluating monitoring trees, we surveyed all overstory trees (> 10 cm DBH) and recruits (2–10 cm DBH) in grid cells where ash occurred between June and September 2022. Our survey protocol consisted of a two-step process. First, we established a 7 m radius plot in the center of each grid cell and demarcated the plot boundary with four stakes set at 7 m from the center. The first stake was set in a random direction from the plot center and the other three stakes were in directions at 90 degree increments. Within the fixed radius plot, we tallied all live and dead recruits by species. Live and dead overstory trees were

also recorded by species and DBH measured. Saplings (trees < 2 cm DBH) and seedlings (< 45 cm height) were not measured.

Next, we established four 18 × 2 m transects that started at the stakes used to delineate the boundary of the fixed-radius plot. Thus, each transect was at a different 90-degree angle from the center and began at the edge of the 7 m fixed radius plot. We walked along these transects and recorded living and dead standing trees by species and DBH class (2–10 cm; then by 5 cm increments). For analysis, we used the mean value of the upper and lower bound of the size class of each tree. Thus, a tree in the 15 – 20 cm class was assigned a DBH of 17.5 cm.

In 2023, we returned to all cells and re-established our 7 m fixed radius plots. We assigned all ash recruits in these plots to one of three EAB infestation classes: 1) alive and infested, 2) alive and apparently uninfested, or 3) dead. Infestation status was based on the presence of new or healed-over EAB galleries, holes left by woodpeckers preying on EAB larvae, or D-shaped adult EAB exit holes.

2.3. Sapling and seedling surveys

In June through September 2023, we quantified seedling and sapling abundance within the previously surveyed grid cells. We defined saplings as trees < 2 cm in diameter and ≥ 45 cm tall, while seedlings were < 45 cm tall. We recorded living and dead saplings within the 7 m fixed-radius plot in the center of each cell. Most saplings were identified to species, but ash were identified only to genus due to the difficulty of differentiating green and white ash saplings. We tallied live tree seedlings by genus within four 1 × 1 m microplots per cell. Each microplot was centered at the stake on the edge of the 7 m radius plot, at 90-degree intervals (Fig. 1). We did not identify nor record dead seedling abundance.

We calculated the area of live ash phloem available to EAB larvae in recruits and overstory trees following McCullough and Siegert (2007). We used the linear equation: "$y = 0.3798x - 1.7587$" (where x is tree DBH) to calculate the phloem area (y) of trees with DBH ≤ 13 cm and the second order polynomial equation "$y = 0.024x^2 - 0.307x + 2.63$" to calculate the phloem area of ash trees > 13 cm. McCullough and Siegert (2007) estimated that, on average, approximately 89 EAB larvae can complete development per square meter of ash phloem area. We used this estimate to calculate the number of beetles that could potentially be supported by the ash phloem area present at our sites. We also calculated the basal area (m^2) of all overstory and recruit-sized trees of each species within each cell using the following equation: $BA(m^2) = \frac{\pi * (\frac{DBH\ in\ cm^2}{2})}{10{,}000}$ which can be simplified to: $BA(m^2) = 0.00007854 * (DBH\ in\ cm)^2$. Basal area of each tree species per hectare within each cell was standardized by dividing the basal area in m^2 by the total area surveyed across the fixed radius plot and all four transects: 0.029794 ha. Sapling densities were standardized on a per hectare basis within each cell by dividing the total stem density by the area of the fixed radius plot (0.015394 ha) and seedling counts were divided by the area of all four microplots (0.0004 ha).

2.4. Statistical analysis

All statistical analyses were conducted in R version 4.3.1 (R Core Team 2023). We used Wilcoxon Rank Sum Tests, also called Mann-Whitney U Tests in the "stats" package to test for differences in canopy dieback and transparency between overstory ash and ash recruits across all field sites and within each site. We also used Wilcoxon Rank Sum Tests to compare density, basal area, and phloem area between living and dead overstory ash and recruits, and to determine if living and dead ash sapling density differed. We used the Benjamini-Hochberg p-value correction procedure to account for Type-I error when testing the effect of tree stratum on canopy dieback and transparency using all sites together and then all sites separately. We used Kruskal-Wallis tests in the "stats" package to determine if the

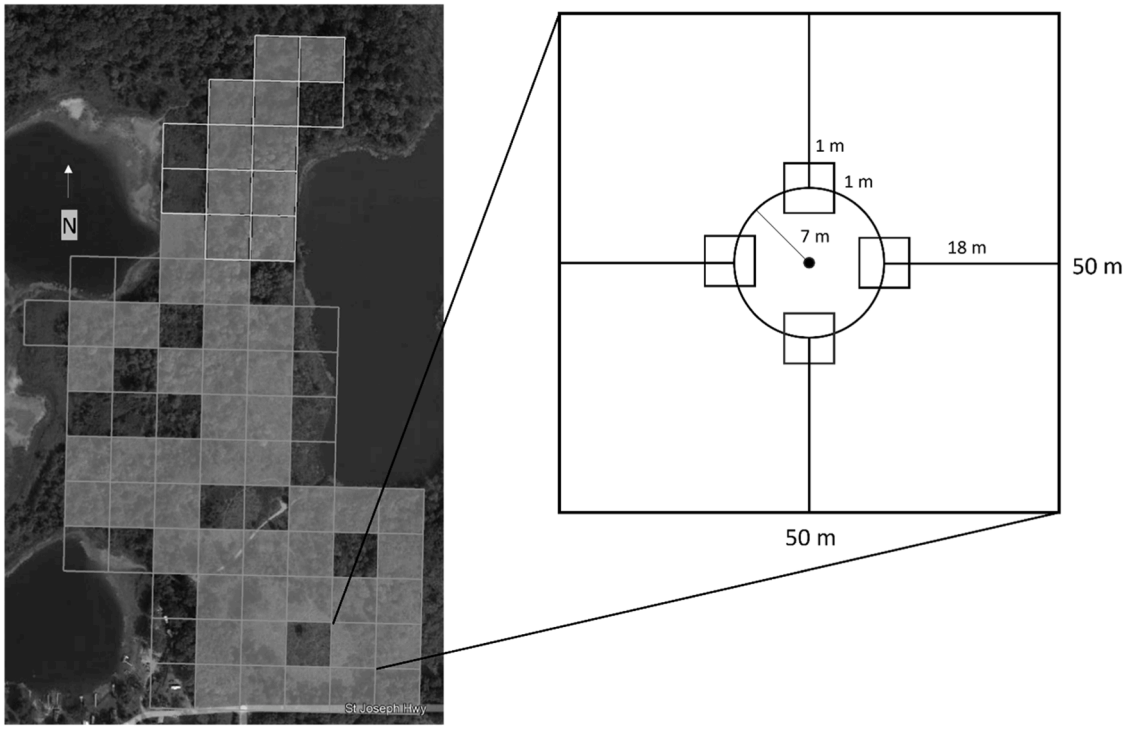

Fig. 1. Left: Satellite view of the Tamarack Lake research area. Highlighted cells had at least four live ash > 3 cm DBH and were used for surveys. Inset: Survey design for each 50 × 50 m grid cell established in the center of each highlighted cell. Within the 7 m fixed radius plot, we recorded overstory trees, recruits, and saplings by species, measured tree (DBH) and tallied recruits as healthy, infested, or dead. At 90-degree intervals along the perimeter, overstory trees and recruits were tallied by DBH size classes along 18 x 2 m linear transects. Four 1 × 1 m microplots were used to quantify seedling density. We recorded percent canopy dieback and transparency on one ash (> 3 cm in DBH) in each direction.

density of living ash stems differed among tree strata (overstory, recruits, saplings, seedlings). If Kruskal-Wallis tests indicated significant effects, we used a post-hoc Dunn test in package "dunn.test" (Dinno and Dinno, 2017) to conduct pair-wise comparisons between strata. We then used the Kruskal-Wallis and Dunn tests to determine if the densities of dead ash stems differed among overstory, recruit, and sapling trees. We used nonparametric tests for these analyses because generalized linear models fit with our data either produced non-normally distributed residuals or exhibited heteroscedasticity.

To determine how the prevalence of ash influenced the composition of overstory and recruit trees (i.e., the community of all trees larger than 2 cm DBH) we used a two-step modelling approach with the package "mvabund" (Wang et al., 2012), which fitted a generalized linear model that determined how a predictor variable influences the composition of a community. Subsequent univariate ANOVAs were used to assess how each species in the community was influenced by the predictor variable (Wang et al., 2012). Using the "manyglm" function, we created a generalized linear model (negative binomial, log-link) that evaluated the effect of live ash basal area (calculated from overstory ash and recruits) on the composition of living trees (stem counts) recorded in our sites. To condense our community data, we excluded tree species represented by less than 10 stems across all grid cells. We performed follow-up univariate tests (using the default p-value adjustment procedure in "many.glm") to assess how live ash basal area influenced the density of each tree species.

3. Results

We recorded data within 178 grid cells (each 50 x 50 m) and we surveyed overstory trees and recruits across 0.029794 ha, saplings across 0.015394 ha, and seedlings across 0.0004 ha within each cell. We surveyed trees within 55 cells at Muskrat Lake, 22 at Rose Lake, 48 at Sleepy Hollow, and 53 at Tamarack Lake. We recorded 365 living overstory ash (73.3 ± 14 stems per ha), 2429 living ash recruits (470.0 ± 68.9 stems per ha), 7316 living ash saplings (2599 ± 336.1 stems per ha), and 322 living ash seedlings (4557 ± 557.9 stems per ha). We recorded 323 dead overstory ash (59.7 ± 3.7 stems per ha), 516 dead ash recruits (100.8 ± 12.8 stems per ha), and 547 dead ash saplings (194.9 ± 56.7 stems per ha). Overall, 47 % of overstory ash stems, 18 % of recruits, and 7 % of saplings were dead.

White ash represented 67 % and 61 % of living and dead overstory ash stems, respectively, while green ash represented 30 % of live overstory ash and 36 % of dead overstory ash. Overstory black ash was only recorded at Tamarack Lake and represented 3 % of living overstory ash and 3 % of dead overstory ash. Density of live and dead overstory white ash stems averaged 54.2 ± 19.6 and 39.2 ± 10.0 stems per ha, while living and dead overstory green ash density averaged 17.7 ± 7.7 and 18.9 ± 7.6 stems per ha. Only nine living and ten dead overstory black ash were recorded at Tamarack Lake, representing 5.7 and 6.3 stems per ha, respectively.

White ash represented 59 % and 62 % of living and dead ash recruit stems respectively, while green ash represented 35 % and 33 % of living and dead ash recruit stems, and black ash represented 6 % and 4 % of living and dead ash recruit stems. Density of live and dead white ash recruits averaged 309.0 ± 105.7 and 68.3 ± 23.1 stems per ha. Living and dead green ash averaged 137.4 ± 59.6 and 28.8 ± 10.2 stems per ha, while living and dead black ash recruits averaged 23.6 ± 22.6 and 3.6 ± 3.4 stems per ha. Black ash recruits were recorded at Muskrat Lake along with Tamarack Lake.

We recorded a total of 8.9 m^2 (1.7 ± 0.2 m^2 per ha) of live ash basal area in overstory trees and 6.9 m^2 (1.3 ± 0.1 m^2 per ha) of live ash basal area in recruits across all cells. Total basal area of dead ash overstory trees and recruits was 9.6 m^2 (1.8 ± 0.2 m^2 per ha) and 1.5 m^2 (0.3 ± 0.03 m^2 per ha), respectively. Total live and dead ash basal area recorded within each cell were not correlated ($t = 0.165$, $df = 176$, $P = 0.869$, $r = 0.012$). However, there was a positive correlation between the percent of the total living and dead tree community's basal area represented by ash and the basal area of standing dead ash ($t = 3.694$, $df = 176$, $P < 0.001$, $r = 0.268$, Fig. S1). Thus, cells with a higher proportion of ash basal area had a greater proportion of that area represented by dead ash. Based on our estimates of overstory and recruit ash basal area, there was a total of 3185 m^2 of live ash phloem area (796.3 ± 131.0 m^2) across all sites which could potentially support 283,465 EAB larvae.

We recorded the condition of all ash recruits present within a 7 m fixed radius plot in each cell. No living or dead ash recruits occurred in plots in 50 cells. In the remaining 128 cells, an average of 33.1 ± 3.0 % of ash recruits were clearly infested by EAB, while 45.5 ± 3.5 % of recruits appeared uninfested and 21.4 ± 2.7 % of ash recruits were dead.

3.1. Canopy condition

In 2022 we assessed canopy dieback and transparency on 712 ash that ranged from 3.0 to 54.6 cm and averaged 12.0 ± 0.3 cm in DBH. We recorded at least one previous or current-year woodpecker attack mark – indicating EAB infestation – on 54 % of overstory ash and 27 % of recruits (Table 1). Current-year seeds were present on 33 % of overstory ash and 14 % of recruits, or 23 % of all ash trees. In 2023, we assessed canopy condition on 709 ash with DBH ranging from 3.0 to 52.7 cm and averaging 12.3 ± 0.3 cm. In 2023, 43 % of overstory and 24 % of recruits had current-year woodpecker attack marks (Table 1). Between canopy assessments conducted in 2022 and 2023 thirty-eight trees died from EAB infestation. These trees averaged 12.3 ± 0.9 cm DBH with 68 ± 4.3 % dieback and 71.1 ± 3.5 % transparency recorded in 2022.

Average dieback for ash of all size classes across all sites was 21.3 ± 0.9 % in 2022 and 24.4 ± 0.9 % in 2023, while canopy transparency averaged 32.3 ± 0.7 %, in 2022 and 35.3 ± 0.7 % in 2023. For overstory ash, canopy dieback averaged 29.3 ± 1.0 % in 2022 and 30.0 ± 1.4 % in 2023, while transparency was 36.5 ± 1.3 % in 2022 and 39.0 ± 1.1 % in 2023. For ash recruits, average dieback was 14.2 ± 1.0 % in 2022 and 18.3 ± 1.0 % in 2023, while transparency was 28.5 ± 0.9 % in 2022 and 31.2 ± 0.8 % in 2023. When all sites were examined together, canopy dieback (2022: $W = 86{,}605$, Adj. $P < 0.001$, 2023: $W = 79{,}046$ Adj. $P < 0.001$) and transparency (2022: $W = 86{,}605$, Adj. $P < 0.001$, 2023: $W = 73{,}935$, Adj. $P < 0.001$) were significantly higher for overstory trees than for recruits in both years (Figs. 2, 3). When sites were analyzed separately, percent dieback was greater for overstory trees than for recruits at Muskrat Lake in 2022 (2022: $W = 7{,}4670$, Adj. $P < 0.001$, 2023: $W = 6414$, Adj. $P = 0.116$), at Rose Lake in 2022 (2022: $W = 1167$, Adj. $P = 0.038$, 2023: $W = 883$, Adj. $P = 0.786$), at Sleepy Hollow in both years (2022: $W = 6151$, Adj. $P < 0.001$, 2023: $W = 6565$, Adj. $P < 0.001$), and at Tamarack Lake in both years (2022: $W = 7125$, Adj. $P < 0.001$, 2023: $W = 7328$, Adj. $P < 0.001$, Fig. 2). Results were generally similar for percent transparency which was significantly greater for overstory trees than recruits

Table 1
Number of living ash across all sites that were evaluated to assess canopy condition including woodpecker attack marks and presence of current-year seeds. In 2022, woodpecker attacks included both current and previous year marks, while in 2023, only current-year attacks are provided.

	2022			2023		
	Overstory	Recruit	Both strata	Overstory	Recruit	Both strata
Total assessed	333	379	712	364	345	709
Trees with woodpecker marks	181	103	284	155	82	237
Trees with current-year seeds	110	52	162	-	-	-

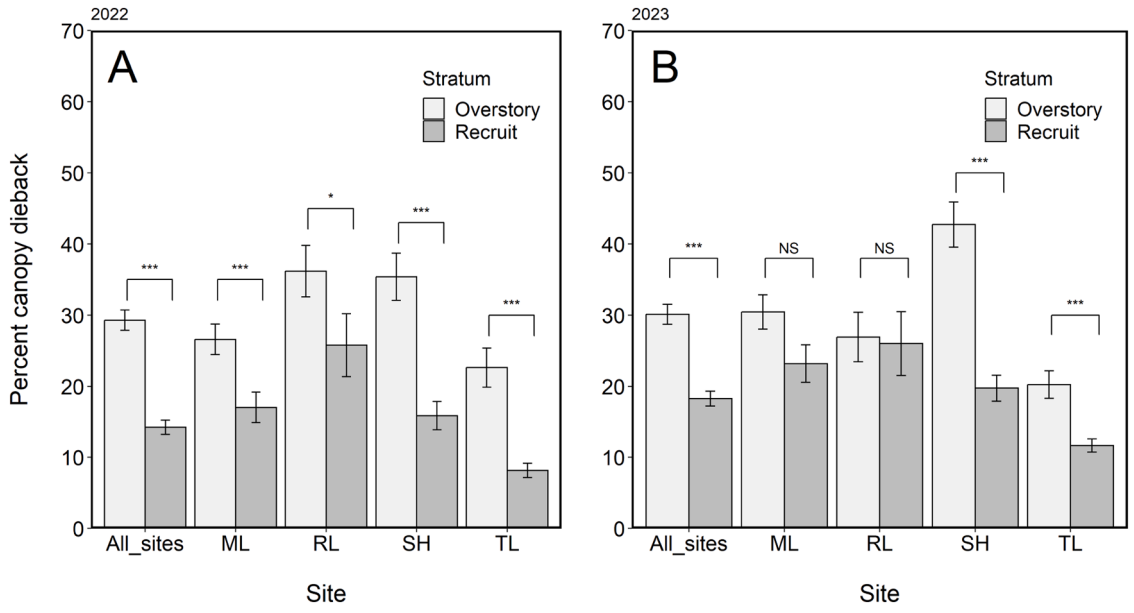

Fig. 2. Average canopy dieback of ash overstory trees and recruits by site and all sites combined for surveys conducted in A) 2022 and B) 2023 at ML: Muskrat Lake, RL: Rose Lake, SH: Sleepy Hollow and TL: Tamarack Lake. In 2023, 38 trees measured in 2022 had died from EAB infestation and 26 died from other disturbances or were unable to be re-located. All dead or lost trees were replaced in 2023. Differences between overstory trees and recruits at each site were evaluated with Wilcoxon Rank Sum Tests. Significance values are represented with asterisks where "* " indicates $P < 0.05$, "* ** " indicates $P < 0.001$ and "NS" indicates $P > 0.05$.

at Sleepy Hollow in both years (2022: W = 5856, Adj. $P < 0.001$, 2023: W = 5556, Adj. $P = 0.002$), but not any other site in either year: Muskrat Lake (2022: W = 6687, Adj. $P = 0.094$, 2023: W = 6546, Adj. P = 0.068), Rose Lake (2022: W = 940, $P = 0.786$, 2023: W = 1068, Adj. $P = 0.068$), Tamarack Lake (2022: W = 4663, Adj. $P = 0.285$, 2023: W = 6083, Adj. $P = 0.114$, Fig. 3). In 2022, 53 overstory ash (16 % of overstory ash) had no dieback and 180 overstory ash (54 %) had < 30 % dieback. In contrast, 147 recruits (43 % of ash recruits) had no dieback, and 308 recruits (82 %) had less than 30 % dieback. In 2023, 41 overstory ash (11 % of overstory ash) had no dieback and 203 overstory ash (56 %) had < 30 % dieback, while 60 recruits had no dieback, (17 % of ash recruits) and 264 recruits (77 %) had < 30 % dieback.

3.2. Density and distribution of ash basal area among strata

Density, basal area, and phloem area of living and dead overstory ash did not significantly differ among sites (Tables 2–3, Figs. 4–5), but were higher for live ash recruits than for dead ash recruits (Tables 2–3, Figs. 4–5). When ash overstory trees and recruits were combined, basal area and phloem area of live ash were significantly higher than those of

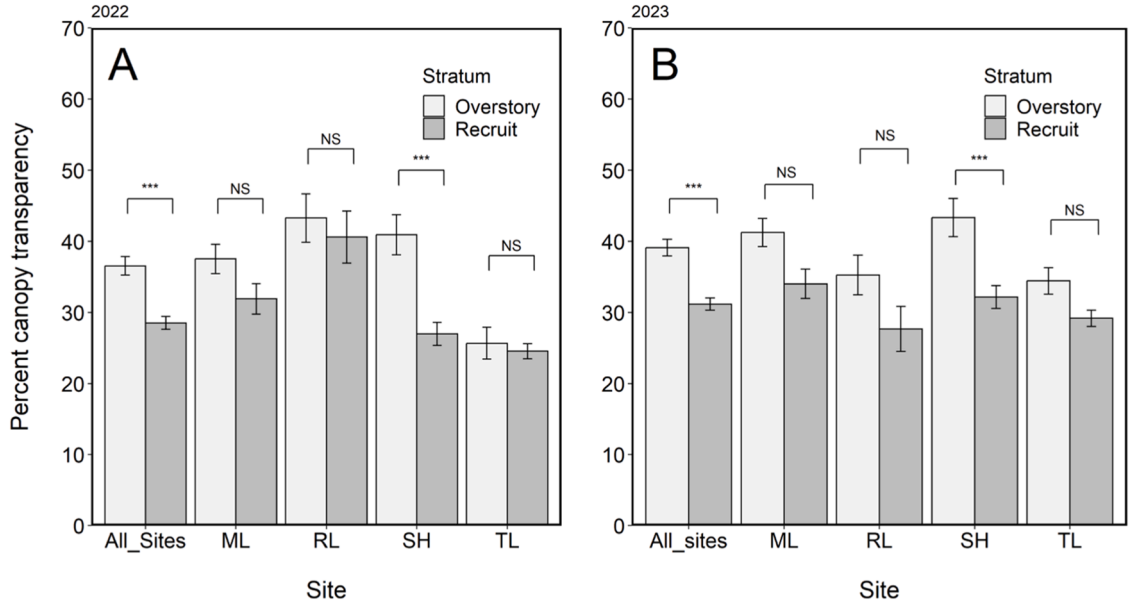

Fig. 3. Average canopy transparency of overstory ash and recruits by site and all sites combined recorded at ML: Muskrat Lake, RL: Rose Lake, SH: Sleepy Hollow and TL: Tamarack Lake for surveys conducted in A) 2022 and B) 2023. In 2023, 38 trees measured in 2022 had died from EAB infestation and 26 died from other disturbances or were unable to be re-located. All dead or lost trees were replaced in 2023. Differences between overstory trees and recruits at each site were evaluated with Wilcoxon Rank Sum Tests. Significance values are represented with asterisks where "* " indicates $P < 0.05$, "* ** " indicates $P < 0.001$, and "NS" indicates $P > 0.05$.

Table 2
Density of live and dead ash (per ha) by stratum followed by live and dead ash basal area (BA) (m^2 per ha) and phloem area (PA) (m^2 per ha) by stratum at each site. Dead ash seedlings were not recorded.

	Live ash				Dead ash			Live ash				Dead ash			
	No. stems per ha				No. stems per ha			Overstory		Recruits		Overstory		Recruits	
Site	Overstory	Recruits	Saplings	Seedlings	Overstory	Recruits	Saplings	BA	PA	BA	PA	BA	PA	BA	PA
Muskrat Lake	85.4	486.4	2545	3843	69.6	119.0	344.4	1.8	381.7	1.4	254.5	1.5	331.8	0.34	63.4
Rose Lake	105.3	572.1	1877	4318	53.4	123.6	153.5	2.2	465.1	1.6	297.6	1.4	295.5	0.35	64.2
Sleepy Hollow	40.6	270.6	3502	6198	61.5	92.3	207.1	1.5	316.2	0.8	140.7	1.4	610.8	0.26	48.0
Tamarack Lake	62.1	551.0	2470	3868	54.5	68.4	74.8	1.6	339.9	1.6	286.6	1.6	314.9	0.20	36.9
All sites	68.8	458.0	2700	4548	60.9	97.3	201.9	1.7	361.9	1.3	238.7	1.8	397.5	0.28	51.5

Table 3
Results of Wilcoxon Rank Sum Tests to assess differences in live and dead ash density, basal area, and phloem area by tree strata. The predictor term in all tests is the status of trees (living or dead).

Response	W	*P*
Overstory ash stems	15,244	0.523
Recruit ash stems	5807	< 0.001
Sapling ash stems	3296	< 0.001
Overstory ash basal area	15,616	0.811
Overstory ash phloem area	15,536	0.745
Recruit ash basal area	5850	< 0.001
Recruit ash phloem area	5868	< 0.001
Overstory and recruit basal area	10,846	< 0.001
Overstory and recruit phloem area	11,039	< 0.001

dead ash (Tables 2–3, Figs. 4–5). We also recorded significantly more living than dead ash saplings (Tables 2–3, Fig. 4B).

Live ash stem density varied among strata (χ^2 = 286.34, df = 3, $P < 0.001$, Table 4, Fig. 4). There were more living ash seedlings (4548 stems per ha) compared to recruits (458 stems per ha), and overstory trees (68.8 stems per ha), although densities of live seedlings (4548 stems per ha) and saplings (2700 stems per ha) did not differ (Table 4). There were also more live ash saplings (2700 stems per ha) compared to recruits (458 stems per ha) and overstory trees (68.8 stems per ha), and more live ash recruits compared to overstory trees (Table 4). Density of dead ash stems also varied among strata ($\chi^2 = 15.438$, df = 2, $P < 0.001$ Table 4). There were more dead ash recruits (97.3 stems per ha) than overstory trees (60.9 stems per ha) and more dead saplings (201.9 stems per ha) than overstory ash; however, densities of dead saplings and dead recruits did not differ (Table 4).

Live ash basal area did not differ between the overstory (1.7 ± 0.2 m^2 per ha) and recruit strata (1.3 ± 0.2 m^2 per ha) (W = 14,118, $P = 0.074$). However, basal area of dead ash was higher for overstory trees (1.8 ± 0.3 m^2 per ha) compared to recruits (0.3 ± 0.04 m^2 per ha) (W = 19,690, $P < 0.001$).

3.3. Tree community composition

Density and basal area of the five most abundant living and dead tree species in each stratum across all sites are listed in Table S1. We recorded a total of 2074 overstory trees of which 78 % were alive. The most common overstory species were *F. americana* (441 stems; 56 % living), *Ulmus americana* (283 stems; 75 % living), *F. pennsylvanica* (228 stems 51 % living), *A. saccharinum* (162 stems; 96 % living), and *Acer negundo* (132 stems 89 % living). We recorded 4994 recruits (84 % living) of which *F. americana* (1760 stems; 82 % living), *F. pennsylvanica* (1013 stems; 83 % living), *U. americana* (625 stems; 83 % living), *Crataegus* spp. (354 stems; 82 % living), and *Carya ovata* (183 stems; 98 % living) were the most common species. Of the 9865 saplings we recorded (87 % alive), *Fraxinus* spp. (7863 stems; 93 % alive), *Prunus serotina* (286 stems; 83 % alive), *Crataegus* spp. (232 stems; 84 % alive), *A. saccharum* (160 stems; 91 % alive), and *U. americana* (159 stems; 86 % alive) were the most common species. Finally, we recorded 654 living seedlings, and *Fraxinus* (322 stems), *Acer* (93 stems), *Prunus* (80

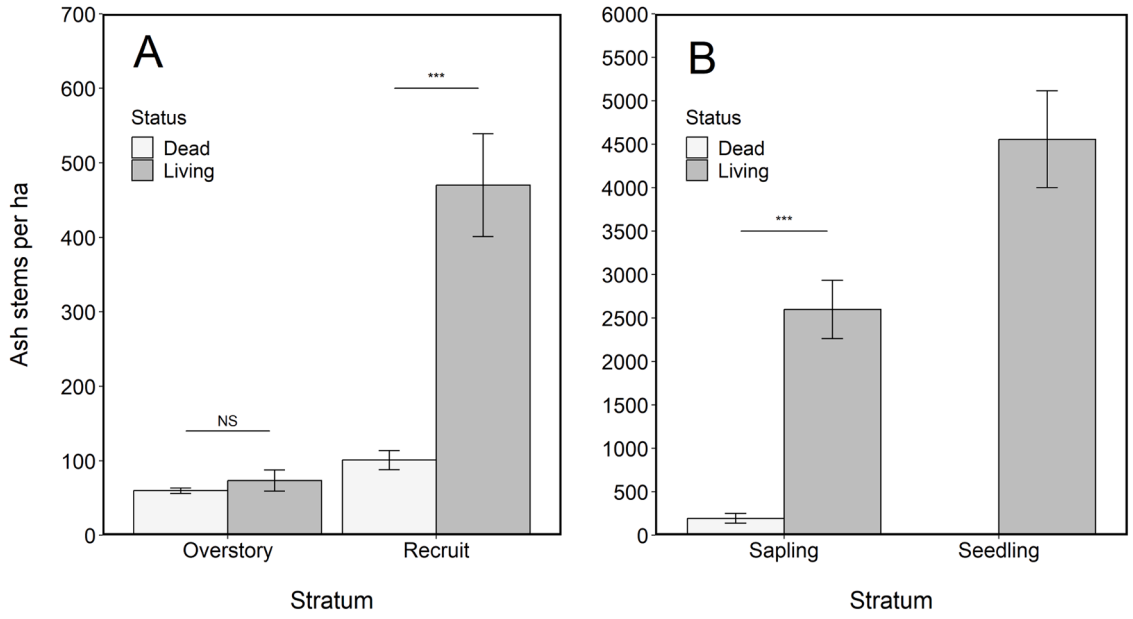

Fig. 4. Number of live and dead ash A) overstory trees and recruits and B) saplings and seedlings per ha recorded across all sites. NS refers to a non-significant differences while "* ** " indicates a *P*-value < 0.001.

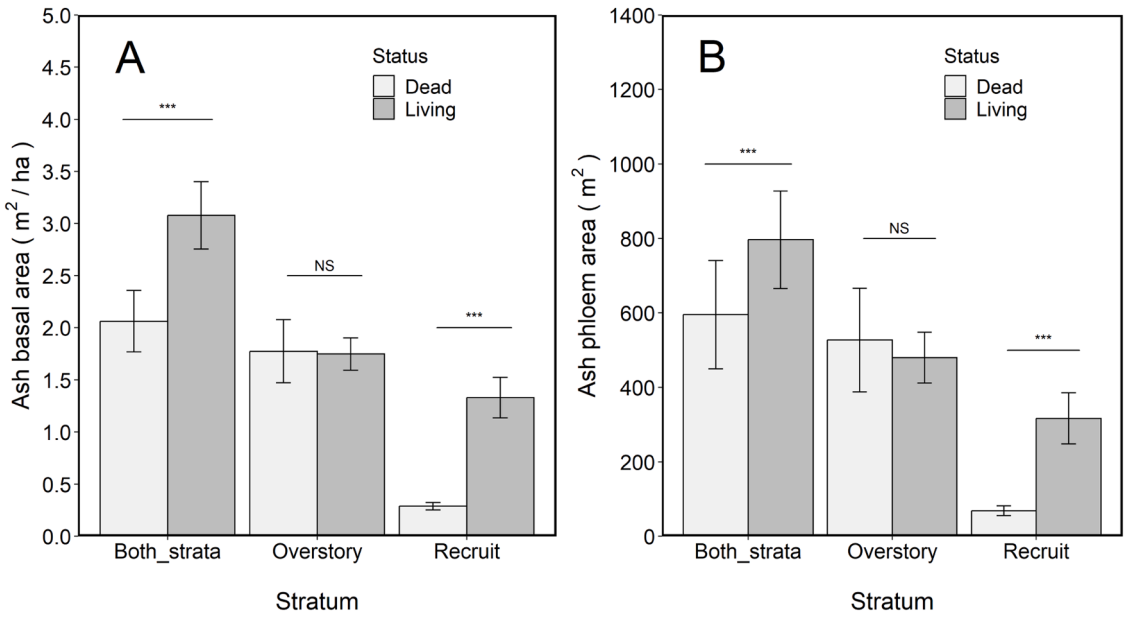

Fig. 5. Distribution of A) ash basal area (m^2 per ha) and B) ash phloem area (m^2) across overstory ash, recruit-sized ash, and both strata combined. NS refers to a non-significant effect while "* ** " indicates $P < 0.001$.

Table 4
Results of Dunn-tests to determine whether density of living and dead stems of each tree stratum differed among other strata. Adjusted *P*-values were calculated with the Benjamini-Hochberg method.

Comparison	Tree condition	Z	Unadjusted *P*	Adjusted *P*
Overstory – recruit	Living	−7.5	< 0.001	< 0.001
Overstory – sapling	Living	−14.0	< 0.001	< 0.001
Recruit – sapling	Living	−6.6	< 0.001	< 0.001
Overstory – seedling	Living	−14.9	< 0.001	< 0.001
Recruit – seedling	Living	−7.4	< 0.001	< 0.001
Sapling – seedling	Living	−0.9	0.394	0.394
Overstory – recruit	Dead	−3.3	0.001	0.001
Overstory – sapling	Dead	−3.5	< 0.001	0.001
Recruit – sapling	Dead	−0.2	NS	NS

stems), *Carya* (55 stems), and *Ulmus* (31 stems) were the most common genera.

3.4. Influence of ash basal area on community composition

When overstory trees and recruits were combined, the amount of live ash basal area was associated with a significant change in tree community composition (Table S2). This effect was driven by changes in the density of *Q. rubra, F. americana,* and *T. americana* associated with changes in ash basal area (Table S2). Not surprisingly, in cells where live ash basal area was low, *F. americana* density was also low, but densities of *Q. rubra* and *T. americana* were high (Fig. 6). In contrast, the summed basal area of dead ash overstory trees and was not related to community composition.

4. Discussion

Documenting current overstory conditions and ash regeneration in post-invasion forests is indicative of the degree to which ash will continue to persist in such stands. Despite the presence of EAB in our

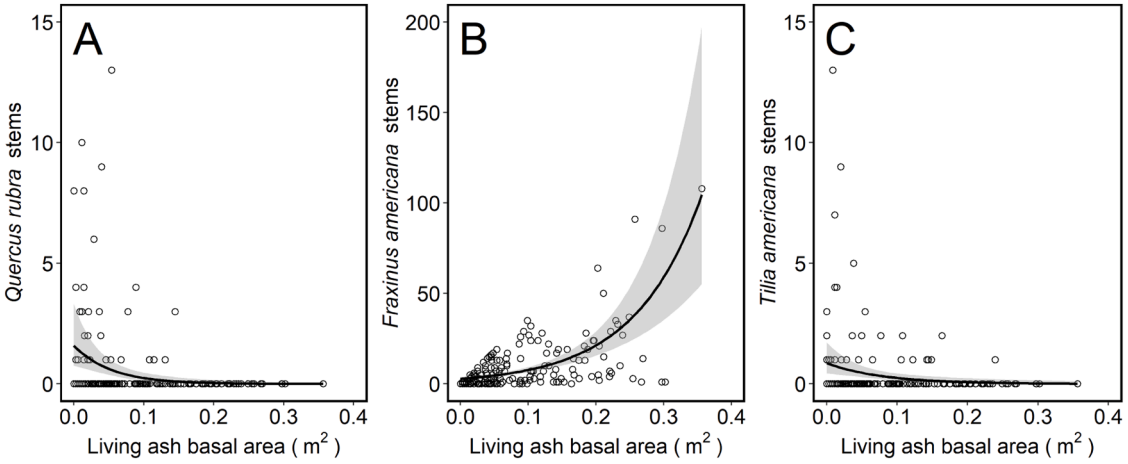

Fig. 6. Cells where live ash basal area was relatively high tended to include A) fewer red oak (*Q. rubra*) stems, B) more white ash (*F. americana*) stems and C) fewer basswood (*T. americana*) stems.

study region for over 20 years, densities of ash recruits, saplings, and seedlings were high relative to other species. However, nearly half (47 %) of the overstory ash encountered in our surveys were dead and approximately one-third of the live ash recruits were infested by EAB. It is unclear what proportion of regenerating ash will be successfully recruited into the overstory and if this value is high enough to support continued reproduction and long-term persistence of ash in post-invasion forests. Moreover, high mortality of overstory ash in our sites suggests an impending loss of seed resources, greater sun exposure, and cascading consequences for forest composition and function (McCullough, 2020). In our upland sites, cells with low ash basal area favored *Q. rubra* and *T. americana* over other tree species, but such relationships were not explained by dead ash basal area. It is therefore unclear how canopy gaps created by EAB-induced ash mortality will alter forest composition. Such effects are likely site specific and will largely depend on what tree species were present prior to EAB invasion.

While ash continues to regenerate in many post-invasion forests in North America, mortality rates remain high, and the extent of overstory ash mortality and ash regeneration appears to vary among ash species (Gould et al., 2022; Kashian et al., 2018; Morris et al., 2023; Siegert et al., 2021). For example, Morris et al. (2023) monitored regeneration and condition of tagged ash trees (half $>$ 10 cm and half $\leq$ 10 cm DBH) in white ash-dominated forests in 2013 and again in 2021 in eastern and western New York. While seedling densities were similar in both sampling periods and locations (ranging from 1000 to 6300 stems per ha), mortality rates of tagged trees (DBH ranging from $<$ 2.5 cm to $>$ 40 cm) were 76 % in eastern New York and 53 % in western New York. In surveys conducted in white ash stands in southeast and central Michigan in 2015–2016, Robinett and McCullough (2019) found an average of 75 % of white ash larger than 10 cm DBH were alive despite more than 10–15 years of EAB presence. They reported average stem densities of ash saplings were 458 $\pm$ 34.3 stems per ha and seedlings were 10,186 $\pm$ 1263 stems per ha. Although it is unclear when our sites were invaded by EAB in comparison to sites studied by Robinett and McCullough (2019), our sites were similarly dominated by white ash, and we recorded high densities of ash saplings (2599 $\pm$ 336.1 stems per ha) and seedlings (4557 $\pm$ 557.9 stems per ha), while 47 % of overstory ash and 17 % of ash recruits were dead. Thus, in the span of approximately 10 years within the same region, regeneration rates remain similar while mortality of overstory trees appears to have increased.

In comparison, recent surveys of post-invasion stands dominated by green ash and/or black ash documented reductions in ash density as high as 99 % and 100 % mortality of trees ($>$ 10 cm DBH) following EAB invasion, and a substantial decline in regenerating ash density (Burr and McCullough, 2014; Engelken and McCullough, 2020b; Kashian, 2016; Klooster et al., 2014; Siegert et al., 2021). White ash is consistently less preferred by EAB than green ash and black ash (Anulewicz et al., 2007; Tanis and McCullough, 2012; 2015). Green ash was present in all our sites and represented 30 % of living overstory ash and 34 % of living ash recruits. Although green ash is colonized sooner and typically sustains greater mortality than white ash, this species has continued to persist in these post-invasion stands. Whether green ash mortality will ultimately exceed recruitment rates in post-invasion stands warrants additional study.

Even when ash is abundant in post-invasion forests, mortality is generally high for trees $>$ 10 cm in diameter and mortality rates increase with tree size (Morris et al., 2023; Robinett and McCullough, 2019; Ward et al., 2021). High mortality of small diameter ash trees could further limit the regeneration potential of ash over time given that white ash can begin flowering when trees are smaller than 10 cm DBH (Schlesinger, 1990) and minimum seed-bearing age ranges from 9 to 20 years (Bonner 2008). When we evaluated canopy condition, seeds were present on 23 % of the ash trees and 32 % of those trees were recruits. In our sites, 46 % of overstory ash and 82 % of ash recruits were relatively healthy with $<$ 30 % canopy dieback, while 47 % of ash overstory trees, 17 % of recruits, and 7 % of saplings were dead. Our data support previous observations that the rate of EAB-caused mortality is higher for larger trees. Using USDA FIA (Forest Inventory and Analysis) data collected in the eastern U.S. in 2002–2007 and 2013–2018, Ward et al. (2021) showed that recruitment of the oldest, and generally largest, ash cohort in the 2013–2018 data was 50 % lower than the mortality rate of this same group. In other words, the largest ash trees were twice as likely to die rather than become incorporated into the overstory canopy. Although our data indicate that ample ash regeneration is occurring where EAB has been established for approximately 10–20 years, it remains unclear if the rate of overstory mortality will eventually outpace regeneration of other strata. Future studies to quantify the percentage of overstory ash and recruits needed to ensure some level of ash regeneration, e.g., ash seedlings and saplings, will help to inform ash conservation efforts.

Ash coarse woody debris (CWD) was present in all our sites but was not measured in this study. Higham et al., (2017) found that standing ash basal area correlated with ash CWD, therefore, grid cells at our sites with high ash basal area may also have ample ash CWD. However, Higham et al., (2017) did not find a clear relationship between CWD and time since EAB invasion within a site, nor with the length time since 25 % of the ash canopy had died. Engelken and McCullough (2020b) measured ash CWD in riparian forests of northwestern Michigan which had been invaded approximately 10 years preceding their surveys and found that 75 % of dead ash were still standing and that most ash CWD was represented by early decay classes. Engelken et al. (2020) tallied standing dead and fallen ash overstory trees killed by EAB in riparian forests across an east-west gradient in southern Michigan. They found that many dead ash had fallen in southeastern sites with the longest history of EAB invasion but standing dead ash were abundant in other sites. Perry et al., (2018) found that ash CWD measured near the epicenter of EAB's invaded range during the initial invasion wave (2004 – 2013) increased by 3.5 % each year once total standing ash basal area had reached 90 % mortality. These studies indicate that there can be a substantial lag time after EAB invasion and overstory mortality before ash CWD represents a significant proportion of ash basal area within a forest stand. Thus, it is unclear how much of the unmeasured ash basal area within our sites is represented by downed trees.

Ash seed production and regeneration may also be limited by other factors. Ash seed weevil [*Lignyoodes helvolus* (LeConte)] may limit the number of successfully germinated seedlings, and dense sedge mats can form in canopy gaps created by ash decline, which subsequently limits seedling germination (Engelken et al., 2020). Although we did not quantify basal-sprout regeneration from top-killed trees in this study, this mode of regeneration can contribute to ash persistence in some areas of Michigan. For example, Kashian (2016) reported that stump sprouts were the dominant form of green ash regeneration in plots surveyed in southeast Michigan from 2010 to 2014 and that 27 % of sprouts produced seeds in 2011, which was a mast year. Whether or not stump-sprouted ash are able to successfully recruit into the overstory has not been studied.

As ash density and phloem have declined following EAB invasion, EAB densities have similarly declined in post-invasion forests. For example, Robinett et al. (2021) found that live ash phloem area explained less than 20 % of the variation in EAB captured on traps placed in post-invasion white ash stands from 2014 to 2016, and that EAB trap captures were similar to levels recorded in recently invaded sites with extremely low EAB densities (e.g. McCullough et al., 2011). They also noted that the canopy condition of trees within their sites generally improved over the study duration, indicating that EAB densities in many of these sites may be low enough to facilitate regeneration. In our sites, estimated live ash phloem area could potentially produce a total of 283,465 EAB adults. When ash trees in our sites were debarked in 2022, EAB densities in declining overstory ash averaged 35.0 $\pm$ 4.3 larvae per m^2 (total of 3059 larvae across 62 declining trees), while in healthy overstory ash, densities averaged 8.6 $\pm$ 13.1 larvae per m^2 (a total of 433 larvae across 62 healthy trees) (Wilson et al., 2024).

While EAB populations have declined substantially across our study region, densities of EAB larvae in these infested trees ash were similar to densities recorded during the initial invasion of EAB into North America (Cappaert et al., 2005, Tluczek et al., 2011). Rates of overstory ash mortality observed at our sites was lower than in other post-invasion forests (Burr and McCullough, 2014; Morris et al., 2023; Siegert et al., 2021; Marshall, 2020), but EAB densities may increase as smaller trees grow to sizes more susceptible to EAB colonization, leading to increased mortality rates. It remains unclear if the population dynamics of EAB and ash will reach a cyclical state of equilibrium, or if ash mortality rates will remain higher than recruitment rates in post-invasion stands.

Species that commonly co-occur with ash such as *U. americana*, *P. serotina*, *Q. rubra*, and *A. rubrum* and *A. saccharum* could fill canopy gaps formed from EAB-induced mortality (Flower et al., 2013; Burr and McCullough, 2014; Engelken et al., 2020; Morris et al., 2023; Robinett and McCullough, 2019; Windmuller-Campione et al., 2021; Marshall, 2020). In our data, *U. americana* was the only non-ash species that occurred at high densities in the overstory, recruit, and sapling strata, and *Ulmus* was also one of the most common seedling genera recorded. *P. serotina* were abundant in the recruit and sapling strata and *Prunus* was a common seedling genus. *A. saccharinum* was common in the overstory while *A. saccharum* was common in the sapling strata, and *Acer* was one of the most common seedling genera. Additionally, *Crataegus* spp. were common in the recruit and sapling strata. While these species may be capable of replacing ash in the overstory, we found that only *Q. rubra* and *T. americana* were more common in cells with lower live ash basal area. However, we also found that no species was influenced by the extent of dead ash basal area, and that live and dead ash basal area were not correlated. Collectively, these findings indicate that reductions in live ash basal area resulting from EAB-induced mortality had little influence on community composition, but rather, cells with low ash basal area may not have been ideal for ash regeneration.

Although EAB remains a devastating pest of ash throughout its invaded range, we have documented substantial regeneration in the recruit, sapling, and seedling strata in four post-invasion forests. The relatively rapid regeneration of ash in post-invasion stands may prevent other tree species from outcompeting and replacing ash in some forests. While EAB densities are lower in post-invasion stands than they are in recently invaded stands, it is unclear how EAB populations will respond as these younger ash cohorts increase in size and if ash recruitment can outpace mortality over time.

Funding

This project was funded by USDA Forest Service Research and Development Target Allocation Grant and USDA Forest Service Northern Research Station and Michigan State University Research Joint Venture Agreement 21-JV-11242303–038.

CRediT authorship contribution statement

McCullough Deborah G.: Writing – review & editing, Supervision, Resources, Project administration, Methodology, Funding acquisition, Conceptualization. **Poland Therese M.:** Writing – review & editing, Supervision, Resources, Project administration, Methodology, Funding acquisition, Conceptualization. **Petrice Toby R.:** Writing – review & editing, Supervision, Resources, Project administration, Methodology, Investigation, Funding acquisition, Conceptualization. **Labbate Louise:** Writing – review & editing, Supervision, Project administration, Methodology, Investigation, Data curation, Conceptualization. **Wilson Caleb J:** Writing – review & editing, Writing – original draft, Visualization, Validation, Supervision, Project administration, Methodology, Investigation, Formal analysis, Data curation, Conceptualization.

Declaration of Competing Interest

The authors do not have any competing interests to declare.

Acknowledgments

We thank the members of the USDA Forest Service lab who assisted with field work: Lindsey Stone, Eric Richard, Adrianna Allen, Julia Zick, Trevor Van Houten, Rachel Dietz, and Nikolas DeWit; as well as members of the MSU Forest Entomology lab who assisted with field work: River Mathieu, Ren McIntyre, Tim Harrison, Drew LaCommare, and Sophia Mota-Chichy. We thank the Michigan Department of Natural Resources for permission to collect data on their properties. Finally, we thank the anonymous reviewers who provided helpful feedback which improved this manuscript.

Appendix A. Supporting information

Supplementary data associated with this article can be found in the online version at doi:10.1016/j.foreco.2025.122546.

Data availability

Data are available for download from figshare: https://doi.org/10.6084/m9.figshare.28303940. Data are also available upon request to the corresponding author.

References

Abella, S.R., Hausman, C.E., Jaeger, J.F., Menard, K.S., Schetter, T.A., Rocha, O.J., 2019. Fourteen years of swamp forest change from the onset, during, and after invasion of emerald ash borer. Biol. Invasions 21 (12), 3685–3696. https://doi.org/10.1007/s10530-019-02080-z.

Anulewicz, A.C., McCullough, D.G., Cappaert, D.L., 2007. Emerald ash borer (*Agrilus planipennis*) density and canopy dieback in three North American ash species. Arboric. Urban For. 33 (5), 338–349. https://doi.org/10.48044/jauf.2007.039.

Aubin, I., Cardou, F., Ryall, K., Kreutzweiser, D., Scarr, T., 2015. Ash regeneration capacity after emerald ash borer (EAB) outbreaks: some early results. For. Chron. 91 (3), 291–298. https://doi.org/10.5558/tfc2015-050.

Aukema, J.E., Leung, B., Kovacs, K., Chivers, C., Britton, K.O., Englin, J., Frankel, S.J., Haight, R.G., Holmes, T.P., Liebhold, A.M., McCullough, D.G., von Holle, B., 2011. Economic impacts of non-native forest insects in the continental United States. PLoS One 6 (9), e24587. https://doi.org/10.1371/journal.pone.0024587.

Bonner, F.T., 2008. *Fraxinus* L. In: Bonner, F.T., Karrfalt, R.P., Nisley, R.G. (Eds.), The woody plant seed manual. U.S. Department of Agriculture Forest Service, Washington, D.C, pp. 537–543.

Burr, S.J., McCullough, D.G., 2014. Condition of green ash (*Fraxinus pennsylvanica*) overstory and regeneration at three stages of the emerald ash borer invasion wave. Can. J. For. Res. 44 (6), 768–776. https://doi.org/10.1139/cjfr-2013-0415.

Cappaert, D., McCullough, D.G., Poland, T.M., Siegert, N.W., 2005. Emerald ash borer in North America: a research and regulatory challenge. Am. Èntomol. 51 (3), 152–165. https://doi.org/10.1093/ae/51.3.152.

Cipollini, D., Morton, E., 2023. The persistence of blue ash in the aftermath of emerald ash borer may be due to adult oviposition preferences and reduced larval performance. Agric. For. Entomol. https://doi.org/10.1111/afe.12582.

Clark, B.F., 1962. White ash, hackberry, and yellow-poplar seed remain viable when stored in the forest litter. Proc. Indiana Acad. Sci. 72, 112–114.

Dinno, A., Dinno, M.A., 2017. Package 'dunn.test'. CRAN Repos. 10, 1–7.

Engelken, P.J., Benbow, M.E., McCullough, D.G., 2020. Legacy effects of emerald ash borer on riparian forest vegetation and structure. For. Ecol. Manag. 457, 117684. https://doi.org/10.1016/j.foreco.2019.117684.

Engelken, P.J., McCullough, D.G., 2020a. Species diversity and assemblages of Cerambycidae in the aftermath of the emerald ash borer (Coleoptera: Buprestidae) invasion in riparian forests of southern Michigan. Environ. Entomol. 49 (3), 391–404. https://doi.org/10.1093/EE/NVAA013.

Engelken, P.J., McCullough, D.G., 2020b. Riparian forest conditions along three northern Michigan rivers following emerald ash borer invasion. Can. J. For. Res. 50 (7), 800–810. https://doi.org/10.1139/cjfr-2019-0387.

ESRI. (2023). *ArcGIS Pro* (v. 3.1.0). Redlands, CA. ⟨https://www.esri.com/en-us/home⟩.

Flower, C.E., Knight, K.S., Gonzalez-Meler, M.A., 2013. Impacts of the emerald ash borer (*Agrilus planipennis* Fairmaire) induced ash (*Fraxinus* spp.) mortality on forest carbon cycling and successional dynamics in the eastern United States. Biol. Invasions 15, 931–944. https://doi.org/10.1007/s10530-012-0341-7.

Godman, R.M., Yawney, H.W., Tubbs, C.H., 1990. *Acer saccharum* Marsh. In: Burns, R.M., Honkala, B.H. (Eds.), Silvics of North America, 2. U.S. Department of Agriculture Forest Service, Washington, D.C, pp. 78–91.

Google Inc. (2022). *Google Earth Pro*. Mountain View, CA. ⟨https://www.google.com/earth/about/⟩.
Gould, J., Fierke, M.K., Hickin, M., 2022. Mortality of emerald ash borer larvae in small regenerating ash in New York forests. J. Econ. Entomol. 115 (4), 1442–1454. https://doi.org/10.1093/jee/toac078.
Grinde, A., Youngquist, M., Slesak, R., Kolbe, S., Bednar, J., Palik, B., D'Amato, A., 2022. Potential impacts of emerald ash borer and adaptation strategies on wildlife communities in black ash wetlands. Ecol. Appl. 32 (1), e02567. https://doi.org/10.1002/eap.2567.
Herms, D.A., McCullough, D.G., 2014. Emerald ash borer invasion of North America: History, biology, ecology, impacts, and management. Annu. Rev. Entomol. 59, 13–30. https://doi.org/10.1146/annurev-ento-011613-162051.
Higham, M., Hoven, B.M., Gorchov, D.L., Knight, K.S., 2017. Patterns of coarse woody debris in hardwood forests across a chronosequence of ash mortality due to the emerald ash borer (*Agrilus planipennis*). Nat. Areas J. 37 (3), 406–411. https://doi.org/10.3375/043.037.0313.
Hoven, B.M., Knight, K.S., Peters, V.E., Gorchov, D.L., 2020. Release and suppression: Forest layer responses to emerald ash borer (*Agrilus planipennis*)-caused ash death. Ann. For. Sci. 77 (1), 27. https://doi.org/10.1007/s13595-019-0895-y.
Kashian, D.M., 2016. Sprouting and seed production may promote persistence of green ash in the presence of the emerald ash borer. Ecosphere 7 (10), e01332. https://doi.org/10.1002/ecs2.1332.
Kashian, D.M., Bauer, L.S., Spei, B.A., Duan, J.J., Gould, J.R., 2018. Potential impacts of emerald ash borer biocontrol on ash health and recovery in southern Michigan. Forests 9 (6), 296. https://doi.org/10.3390/f9060296.
Kashian, D.M., Witter, J.A., 2011. Assessing the potential for ash canopy tree replacement via current regeneration following emerald ash borer-caused mortality on southeastern Michigan landscapes. For. Ecol. Manag. 261 (3), 480–488. https://doi.org/10.1016/j.foreco.2010.10.033.
Klooster, W.S., Gandhi, K.J.K., Long, L.C., Perry, K.I., Rice, K.B., Herms, D.A., 2018. Ecological impacts of emerald ash borer in forests at the epicenter of the invasion in North America. Forests 9 (5), 250. https://doi.org/10.3390/f9050250.
Klooster, W.S., Herms, D.A., Knight, K.S., Herms, C.P., McCullough, D.G., Smith, A., Gandhi, K.J.K., Cardina, J., 2014. Ash (*Fraxinus* spp.) mortality, regeneration, and seed bank dynamics in mixed hardwood forests following invasion by emerald ash borer (*Agrilus planipennis*). Biol. Invasions 16 (4), 859–873. https://doi.org/10.1007/s10530-013-0543-7.
Knight, K.S., Brown, J.P., Long, R.P., 2013. Factors affecting the survival of ash (Fraxinus spp.) trees infested by emerald ash borer (*Agrilus planipennis*). Biol. Invasions 15 (2), 371–383. https://doi.org/10.1007/s10530-012-0292-z.
Kolka, R.K., D'Amato, A.W., Wagenbrenner, J.W., Slesak, R.A., Pypker, T.G., Youngquist, M.B., Grinde, A.R., Palik, B.J., 2018. Review of ecosystem level impacts of emerald ash borer on black ash wetlands: what does the future hold? Forests 9 (4), 179. https://doi.org/10.3390/f9040179.
Krzemien, S., Robertson, W.M., Engelken, P.J., McCullough, D.G., 2024. Observations of reduced ET and persistent elevated water table beneath a riparian forest gap following emerald ash borer invasion and tree mortality. Hydrol. Process. 38 (4), e15117. https://doi.org/10.1002/hyp.15117.
Larson, C.E., Engelken, P., McCullough, D.G., Benbow, M.E., 2022. Emerald ash borer invasion of riparian forests alters organic matter and bacterial subsidies to south Michigan headwater streams. Can. J. Fish. Aquat. Sci. 79 (2), 298–312. https://doi.org/10.1139/cjfas-2022-0127.
Marquis, D.A., 1990. *Prunus serotina* Ehrh. Black Cherry. In: Burns, R.M., Honkala, B.H. (Eds.), Silvics of North America, 2. U.S. Department of Agriculture Forest Service, Washington, D.C, pp. 594–604.
Marshall, J.M., 2020. Forest compositional changes after a decade of emerald ash borer. Forests 11 (9), 949. https://doi.org/10.3390/f11090949.
McCullough, D.G., 2020. Challenges, tactics and integrated management of emerald ash borer in North America. Forestry 93 (2), 197–211. https://doi.org/10.1093/forestry/cpz049.
McCullough, D.G., Siegert, N.W., 2007. Estimating potential emerald ash borer (Coleoptera: Buprestidae) populations using ash inventory data. J. Econ. Entomol. 100 (5), 1577–1586. https://doi.org/10.1603/0022.
McCullough, D.G., Siegert, N.W., Poland, T.M., Pierce, S.J., Ahn, S.Z., 2011. Effects of trap type, placement and ash distribution on emerald ash borer captures in a low density site. Environ. Entomol. 40 (5), 1239–1252. https://doi.org/10.1603/EN11099.
Morris, T.D., Gould, J.R., Drake, J., Fierke, M.K., 2023. Status of ash forests and regeneration a decade after first detection of emerald ash borer infestation in New York state. For. Ecol. Manag. 549, 121464. https://doi.org/10.1016/j.foreco.2023.121464.
Nisbet, D., Kreutzweiser, D., Sibley, P., Scarr, T., 2015. Ecological risks posed by emerald ash borer to riparian forest habitats: a review and problem formulation with management implications. For. Ecol. Manag. 358, 165–173. https://doi.org/10.1016/j.foreco.2015.08.030.
Perry, K.I., Herms, D.A., Klooster, W.S., Smith, A., Hartzler, D.M., Coyle, D.R., Gandhi, K. J., 2018. Downed coarse woody debris dynamics in ash (*Fraxinus* spp.) stands invaded by emerald ash borer (*Agrilus planipennis* Fairmaire). Forests 9 (4), 191. https://doi.org/10.3390/f9040191.
R Core Team, 2023. R: A language and environment for statistical computing. R Foundation for Statistical Computing, Vienna, Austria. ⟨https://www.R-project.org/⟩.
Robinett, M.A., McCullough, D.G., 2019. White ash (*Fraxinus americana*) survival in the core of the emerald ash borer (*Agrilus planipennis*) invasion. Can. J. For. Res. 49 (4), 510–520. https://doi.org/10.1139/cjfr-2018-0320.
Robinett, M.A., Poland, T.M., McCullough, D.G., 2021. Captures of emerald ash borer (*Agrilus planipennis*) adults in post-invasion white ash sites with varying amounts of live phloem. Forests 12 (3), 262. https://doi.org/10.3390/f12030262.
Schlesinger, R.C., 1990. *Fraxinus americana* L. White ash. In: Burns, R.M., Honkala, B.H. (Eds.), Silvics of North America, 2. U.S. Department of Agriculture Forest Service, Washington, D.C, pp. 333–338.
Shoemaker, M.E., Zarnoch, S.J., Bechtold, W.A., Latelle, D.J., Burkman, W.G., & Cox, S. M. (2007). *Crown-condition classification: A guide to data collection and analysis*. U.S. Department of Agriculture Forest Service, Southern Research Station, General Technical Report SRS-102.
Siegert, N.W., Engelken, P.J., McCullough, D.G., 2021. Changes in demography and carrying capacity of green ash and black ash ten years after emerald ash borer invasion of two ash-dominant forests. For. Ecol. Manag. 494, 119335. https://doi.org/10.1016/j.foreco.2021.119335.
Smith, A., Herms, D.A., Long, R.P., Gandhi, K.J.K., 2015. Community composition and structure had no effect on forest susceptibility to invasion by the emerald ash borer (Coleoptera: Buprestidae). Can. Èntomol. 147 (3), 318–328. https://doi.org/10.4039/tce.2015.8.
Smitley, D., Davis, T., Rebek, E., 2008. Progression of ash canopy thinning and dieback outward from the initial infestation of emerald ash borer (Coleoptera: Buprestidae) in southeastern Michigan. J. Econ. Entomol. 101 (5), 1643–1650. https://doi.org/10.1093/jee/101.5.1643.
Spei, B.A., Kashian, D.M., 2017. Potential for persistence of blue ash in the presence of emerald ash borer in southeastern Michigan. For. Ecol. Manag. 392, 137–143. https://doi.org/10.1016/j.foreco.2017.02.053.
Tanis, S.R., McCullough, D.G., 2012. Differential persistence of blue ash and white ash following emerald ash borer invasion. Can. J. For. Res. 42 (8), 1542–1550. https://doi.org/10.1139/X2012-103.
Tanis, S.R., McCullough, D.G., 2015. Host resistance of five Fraxinus species to *Agrilus planipennis* (Coleoptera: Buprestidae) and effects of paclobutrazol and fertilization. Environ. Entomol. 44 (2), 287–299. https://doi.org/10.1093/ee/nvu005.
Tluczek, A.R., McCullough, D.G., Poland, T.M., 2011. Influence of tree size and canopy position on the severity of emerald ash borer (*Agrilus planipennis*) attacks in urban trees. J. Econ. Entomol. 104 (4), 1125–1132. https://doi.org/10.1603/EC10468.
Walters, R.S., Yawney, H.W., 1990. Acer rubrum L. Red Maple. In: Burns, R.M., Honkala, B.H. (Eds.), Silvics of North America, 2. U.S. Department of Agriculture Forest Service, Washington, D.C., pp. 60–69
Wang, Y.I., Naumann, U., Wright, S.T., Warton, D.I., 2012. mvabund–an R package for model-based analysis of multivariate abundance data. Methods Ecol. Evol. 3 (3), 471–474. https://doi.org/10.1111/j.2041-210X.2012.00190.x.
Ward, S.F., Liebhold, A.M., Morin, R.S., Fei, S., 2021. Population dynamics of ash across the eastern USA following invasion by emerald ash borer. For. Ecol. Manag. 479, 118574. https://doi.org/10.1016/j.foreco.2020.118574.
Wilson, C.J., Petrice, T.R., Poland, T.M., McCullough, D.G., 2024. Tree species richness and ash density have variable effects on emerald ash borer biological control by woodpeckers and parasitoid wasps in post-invasion white ash stands. Environ. Entomol. 53 (4), 544–560. https://doi.org/10.1093/ee/nvae060.
Windmuller-Campione, M.A., Russell, M.B., Slesak, R.A., Lochner, M., 2021. Regeneration responses in black ash (Fraxinus nigra) wetlands: implications for forest diversification to address emerald ash borer (Agrilus planipennis). New For. 52, 537–558. https://doi.org/10.1007/s11056-020-09807-0.